nature structural & molecular biology

Molecular mechanisms for protein-encoded inheritance

Jed J W Wiltzius[1,3], Meytal Landau[1,3], Rebecca Nelson[1,3], Michael R Sawaya[1,3], Marcin I Apostol[1,3], Lukasz Goldschmidt[1], Angela B Soriaga[1], Duilio Cascio[1], Kanagalaghatta Rajashankar[2] & David Eisenberg[1]

In prion inheritance and transmission, strains are phenotypic variants encoded by protein 'conformations'. However, it is unclear how a protein conformation can be stable enough to endure transmission between cells or organisms. Here we describe new polymorphic crystal structures of segments of prion and other amyloid proteins, which offer two structural mechanisms for the encoding of prion strains. In packing polymorphism, prion strains are encoded by alternative packing arrangements (polymorphs) of β-sheets formed by the same segment of a protein; in segmental polymorphism, prion strains are encoded by distinct β-sheets built from different segments of a protein. Both forms of polymorphism can produce enduring conformations capable of encoding strains. These molecular mechanisms for transfer of protein-encoded information into prion strains share features with the familiar mechanism for transfer of nucleic acid–encoded information into microbial strains, including sequence specificity and recognition by noncovalent bonds.

Prions are infectious proteins that, in mammals, give rise to transmissible neurodegenerative diseases[1] and, in fungi, produce heritable and sometimes beneficial phenotypes[2,3]. Although distinctly different in sequence and cellular role, the mammalian and most fungal prion proteins share similarities in their mechanisms of formation and propagation[2,4]. Prion formation involves a structural conversion in which the protein changes from its normal, soluble structure to an aggregated, amyloid-like structure rich in β-sheets. This conversion involves breaking intramolecular noncovalent bonds and forming intermolecular hydrogen bonds and other noncovalent bonds. The resulting prion aggregates then seed the conversion of identical soluble protein molecules to the aggregated state. Mammalian and fungal prions also share the phenomenon of strains, in which structural conversions of the same protein give rise to different disease characteristics or phenotypes[2]. Although mammalian disease strains show a correlation with differences in prion conformation[5–7], the causal link has been proven in yeast: distinct conformations of aggregated Sup35 give rise to distinct strains of *[PSI$^+$]*[8,9].

Amyloid fibrils, though not generally infectious, share with prion aggregates their cross-β-spine structure and a propensity for conformational variation, or polymorphism. Amyloid conformers give rise to fibrils with distinct properties, such as NMR spectra[10] and morphology[10,11]—for example, twisted versus flat fibrils, or fibrils of different widths. Similar morphologies have been observed for *in vitro*–formed mammalian prion fibrils[12], suggesting commonalities between the conformational differences that produce amyloid fibril polymorphism and those that give rise to prion strains. The observation that an amyloid disease is transmissible in mice[13] further blurs the distinction between amyloid and prion.

Despite pioneering studies[14–19], little is known at the atomic level about the nature of the conformational differences that give rise to polymorphic amyloid fibrils and prion strains. In our previous work, we determined 13 fibril-like structures of segments from proteins known to fibrillize; these structures consist of pairs of tightly packed, highly complementary β-sheets[20,21], which we termed 'steric zippers'. Each steric zipper is formed from identical short segments of protein molecules, stacked into β-sheets that run the entire length of the amyloid-like fibrils, and of the closely-related needle-shaped microcrystals[21,22] used to determine the atomic structures of the steric zippers. These steric zippers include three polymorphic pairs (alternative packing arrangements) that might be connected to the phenomenon of prion strains. Since then, in the course of determining new fibril-like structures, we have found that polymorphic structures are common among steric zippers. Here we present nine new structures that include three distinct types of polymorphs, and we present the structural and biochemical arguments indicating that the conformational differences of prion strains may be attributable to polymorphic steric zippers. We also discuss the similarities in information transfer between protein-encoded prion inheritance and the more familiar nucleic acid–encoded inheritance.

RESULTS

Packing polymorphism of steric zippers

In determining the atomic structures of steric zippers by X-ray microcrystallography, including the nine new structures reported here (**Tables 1** and **2** and **Supplementary Table 1**), we found that some segments of amyloid and prion proteins form two packing types, or polymorphs. Four such pairs are shown in **Figure 1**. The fibril-forming segment[22] SSTNVG is derived from islet amyloid

[1]UCLA-DOE Institute for Genomics and Proteomics, Howard Hughes Medical Institute, Molecular Biology Institute, University of California, Los Angeles, California, USA. [2]NE-CAT and Department of Chemistry and Chemical Biology, Cornell University, Argonne National Laboratory, Argonne, Illinois, USA. [3]These authors contributed equally to this work. Correspondence should be addressed to D.E. (david@mbi.ucla.edu).

Received 17 April; accepted 17 June; published online 16 August 2009; doi:10.1038/nsmb.1643

Table 1 Data collection and refinement statistics for structures in Figure 1

	SSTNVG form 2	VQIVYK form 2	NNQNTF
Data collection			
Space group	$P2_12_12_1$	$C2$	$P2_1$
Cell dimensions			
a, *b*, *c* (Å)	16.59, 4.79, 40.23	28.64, 4.88, 35.81	18.06, 4.84, 21.36
α, β, γ (°)	90.0, 90.0, 90.0	90.0, 110.5, 90.0	90.0, 100.1, 90.0
Resolution (Å)	1.6	1.5	1.45
R_{merge} (%)	14.9 (49.9)	16.0 (37.6)	13.7 (27.3)
$I/\sigma I$	6.5 (1.3)	8.1 (4.7)	7.2 (3.4)
Completeness (%)	92.6 (85.7)	94.4 (82.1)	98.7 (100.0)
Redundancy	4.5 (2.8)	4.1 (4.0)	5.4 (4.3)
Refinement			
Resolution (Å)	20.11–1.61 (1.80–1.61)	33.54–1.51 (1.68–1.51)	21.0–1.46 (1.46–1.50)
No. reflections	503 (78)	825 (156)	707 (40)
R_{work}/R_{free}	22.3/25.3 (26.5/39.6)	17.4/19.6 (19.6/27.0)	16.2/17.4 (23.6/39.6)
No. atoms			
Protein	39	58	52
Water	3	1	2
B-factors			
Protein	8.6	6.8	0.7
Water	22.2	26.0	2.0
r.m.s. deviations			
Bond lengths (Å)	0.004	0.007	0.007
Bond angles (°)	0.91	1.03	0.77

One crystal was used for each data set. Values in parentheses are for highest-resolution shell.

polypeptide (IAPP), a 37-residue hormone that forms fibrillar amyloid deposits among the pancreatic β-islet cells of nearly all type II diabetics[23]. Microcrystals of SSTNVG grown from different solutions revealed two structures (polymorphs), one featuring a pair of serine residues at the center (**Fig. 1a**, left)[22], and the other, with a shifted registration of the two β-sheets, featuring a pair of asparagine residues at the center (**Fig. 1a**, right). In both polymorphs, a pair of tightly interdigitated β-sheets, with no water molecules in the interface, forms the basic dry steric zipper structure. A second pair of polymorphic steric zippers is formed by the segment VQIVYK (**Fig. 1b**) from the fibril-forming protein tau, associated with Alzheimer's disease[24]. Again, microcrystals grown under different conditions (**Supplementary Methods**) produced different structures related by a shift in registration of the two sheets. These two pairs of polymorphs of segments SSTNVG and VQIVYK show that a given fibril-forming sequence can form distinct steric zippers by adopting distinct registrations of the two β-sheets. We term this 'registration polymorphism'.

Two additional pairs of steric zippers (**Fig. 1c**,**d**), one from the fibril-forming segment NNQQ of the yeast prion Sup35 (ref. 21) and the other from the segment NNQNTF of elk prion protein associated with strains[25], revealed what we term 'facial polymorphism'. In the steric zippers on the right, the two sheets are packed face to face, as in SSTNVG and VQIVYK. The steric zippers on the left are packed face to back (NNQQ) or back to back (NNQNTF).

Each of the eight steric zippers in **Figure 1** seems stable and is likely to be separated from its alternative polymorph by a high energy barrier. Each β-sheet of a zipper is stabilized by main chain hydrogen bonds between layers. The two sheets of a zipper are held together by van der Waals bonds between the highly complementary, interdigitated side chains, and in a few cases by intersheet hydrogen bonds, as in the left polymorph of SSTNVG (**Fig. 1a**). To transform one polymorph into another, it is necessary to break the intersheet contacts, reposition the two sheets and reinterdigitate the side chains to form the second zipper. The high energy barrier presented by bond breaking means that the two polymorphs are distinct, stable, long-lived structures.

Segmental polymorphism in steric zippers of IAPP

The amyloid-forming protein IAPP shows a rich variety of fibril morphologies[11,18]. IAPP also shows a rich variety of steric zippers: six different segments of the IAPP sequence form distinct amyloid-like fibrils and microcrystals (**Fig. 2**). Rather than different packing arrangements of the same segment, as described above, each of these

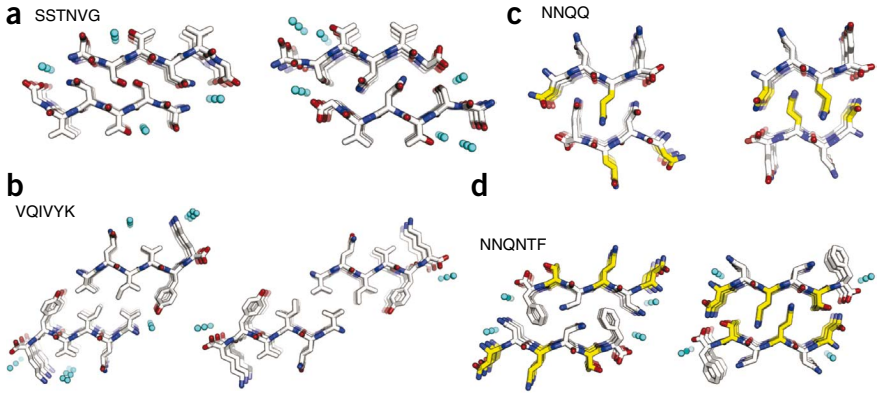

Figure 1 Packing polymorphism of steric zippers, determined by X-ray microcrystallography. A steric zipper is a pair of interdigitated β-sheets, generally with a dry interface between them. The views here look down the fibril axes, showing three layers of the zipper. In actual fibrils and microcrystals, there are tens of thousands of layers. Each strand forms backbone hydrogen bonds to strands above and below it. Water molecules are shown as aqua spheres. (**a**) Registration polymorphism of SSTNVG from IAPP. The left steric zipper (PDB code 3DG1; ref. 22) can be transformed to the right steric zipper by moving the top sheet to the left and flipping side chains S2 and N4. (**b**) Registration polymorphism of VQIVYK from tau protein. The left zipper (PDB code 2ON9; ref. 21) can be transformed to the right zipper by moving the top sheet to the right. (**c**) Facial polymorphism of NNQQ from yeast prion Sup35. The left NNQQ steric zipper (PDB code 2ONX; ref. 21) shows face-to-back packing, with the N1 and Q3 amino acid side chains (yellow) of the top sheet interdigitated with the Q4 and N2 (white) of the bottom sheet. In contrast, the right NNQQ steric zipper (PDB code 2OLX; ref. 21) shows face-to-face packing, with the N1 and Q3 side chains (yellow) of both sheets forming the interdigitated interface. (**d**) Facial polymorphism of NNQNTF from elk prion protein[25]. Both NNQNTF steric zippers are found in the same crystal structure, one face to face (right), with N1, Q3 and T5 (yellow) of both sheets forming the interdigitated interface, and the other back to back, with side chains N2, N4 and F6 interdigitated (white).

Table 2 Data collection and refinement statistics for structures in Figure 2

	NFLVHS	NFLVHSS	HSSNNF	AILSST	NVGSNTY form 1	NVGSNTY form 2
Data collection						
Space group	$P2_12_12_1$	$P2_1$	$P2_1$	$P2_1$	$P2_1$	$P2_1$
Cell dimensions						
a, *b*, *c* (Å)	9.55, 11.48, 38.58	9.73, 21.60, 26.09	4.82, 16.39, 23.48	9.54, 86.65, 19.48	20.63, 4.70, 21.01	20.65, 4.82, 29.05
α, β, γ (°)	90.0, 90.0, 90.0	90.0, 95.6, 90.0	90.0, 92.5, 90.0	90.0, 90.0, 90.0	90.0, 92.3, 90.0	90.0, 101.3, 90.0
Resolution (Å)	1.85	1.84	1.50	1.40	1.50	1.60
R_{merge} (%)	18.3 (41.9)	18.9 (46.0)	15.9 (57.2)	17.5 (55.9)	18.9 (39.2)	15.5 (49.0)
$I/\sigma I$	7.3 (2.5)	5.7 (2.2)	9.5 (3.7)	8.3 (2.0)	6.2 (2.2)	6.6 (2.7)
Completeness (%)	93.9 (82.9)	95.2 (89.1)	93.6 (75.6)	84.5 (85.5)	95.0 (86.5)	95.7 (94.0)
Redundancy	5.4 (6.4)	2.8 (2.8)	4.3 (4.4)	2.7 (2.5)	5.2 (2.8)	3.1 (3.1)
Refinement						
Resolution (Å)	19.29–1.85 (1.90–1.85)	25.97–1.84 (1.89–1.84)	23.45–1.50 (1.68–1.50)	43.31–1.40 (1.44–1.40)	20.99–1.50 (1.67–1.50)	28.51–1.60 (1.78–1.60)
No. reflections	379 (26)	825	509	4723	662	984
R_{work}/R_{free}	19.2/23.2 (29.5/26.9)	23.8/28.2 (25.5/21.6)	17.3/20.7 (20.4/21.2)	22.2/26.5 (30.8/34.9)	14.8/15.8 (19.9/27.7)	12.4/15.9 (17.8/23.1)
No. atoms						
Protein	51	124	50	328	53	318
Ligand/ion	1	5	0	0	0	0
Water	1	7	4	67	5	0
B-factors						
Protein	13.5	6.7	4.2	11.8	3.9	2.5
Ligand/ion	69.9	33.1	—	—	—	—
Water	32.7	17.2	20.4	24.3	7.1	—
r.m.s. deviations						
Bond lengths (Å)	0.005	0.016	0.004	0.003	0.006	0.009
Bond angles (°)	0.61	1.56	0.70	0.79	1.12	1.66

Four crystals were used for NVGSNTY form 1. Two crystals were used for NFLVHSS. One crystal was used for each of the remaining data sets. Values in parentheses are for highest-resolution shell.

polymorphic steric zippers is formed from a different segment of the IAPP sequence (**Supplementary Figs. 1–3**).

The six IAPP segments in **Figure 2** form fibrils and needle-shaped microcrystals suitable for X-ray diffraction studies. Each of the six microcrystals reveals a distinctive steric zipper structure. We expected fibrils and microcrystals formed by the same segment to have similar structures, because fibrils and microcrystals often grow under the same conditions (see the micrograph of NNFGAIL fibrils, **Fig. 2**); in both, the extended segment is perpendicular to the long axis, with the β-sheets parallel to the axis; both give characteristic amyloid diffraction peaks at ~10 Å and 4.7 Å (ref. 26); and occasionally we find fibrils that seem to emanate from the tips of microcrystals (see the micrograph of HSSNNF fibrils, **Fig. 2**). In short, six segments of one protein, IAPP, form six fibril-like structures, each differing from all of the others at the atomic level, a striking segmental polymorphism.

Full-length IAPP forms distinct steric zippers

Our biochemical studies of human and mouse IAPP show that the spines of full-length IAPP fibrils can be built from steric zippers of at least two different segments. Human IAPP forms fibrils of several morphologies[11,18], whereas mouse IAPP does not form fibrils[27] (**Fig. 3a**). The established involvement of the C-terminal region (residues 21–37) in human IAPP fibrillization[28] is reinforced by differences in the human and mouse sequences (**Fig. 2a** and **Supplementary Fig. 4**); five of the six residue differences are in the C-terminal region.

We found that the N-terminal region of IAPP (residues 1–20) is also sufficient to drive fibrillization. Replacement of Arg18 in mouse IAPP with histidine (R18H), as in human IAPP, impart fibril-forming ability to mouse IAPP, although these fibrils form more slowly than those of human IAPP[29] (**Fig. 3a**). Also, the pH profile of mouse IAPP R18H fibril formation shows an inflection at pH 6 (**Supplementary Fig. 5**), roughly the pK_a of the substituted histidine, further implicating His18 in fibrillization (**Fig. 3b**). The C-terminal region of mouse IAPP R18H is not responsible for fibrillation because of the mouse substitutions that prevent fibrillation (**Fig. 2a**). Moreover, the fibrils of human IAPP and mouse IAPP R18H differ in morphology (**Fig. 3c**). A further experiment suggested that a segment within the C terminus preferentially forms the spine within full-length human IAPP. In this experiment (**Fig. 3a**), substitution of the mouse residue into human IAPP at position 18 (H18R) did not affect the kinetics of fibril formation (**Fig. 3a**). It did, however, lower the fluorescence maximum, perhaps as a result of lower ThT binding, perhaps from alternative packing of protofibrils into fibrils.

Thus, the human IAPP sequence contains at least two fragments capable of forming amyloid cross–β spines: the C-terminal region, with a high propensity to form a zipper spine, and a kinetically less favorable segment within the N-terminal region containing His18 (**Fig. 3a**). The formation of a steric zipper within either region would preclude the formation of a steric zipper within the other region of the same molecule. Considering this result in light of the structures in **Figure 2**, we conclude that full-length IAPP can form polymorphs based on segmental polymorphism at the atomic level.

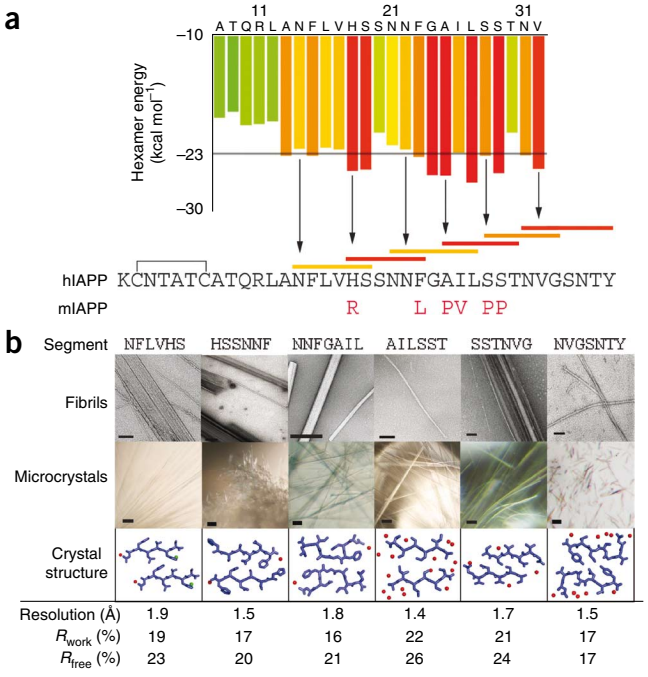

Figure 2 Segmental polymorphism in IAPP. (**a**) IAPP sequences and segment propensities for fibril formation. The sequence of human IAPP (hIAPP) is shown below, with residue replacements in mouse IAPP (mIAPP) underneath. The histogram above shows the estimated energies of steric zippers formed by six-residue segments (starting at the listed residue) of IAPP. Segments having energies of –23 kcal mol^{-1} or lower are predicted to form fibrils[42]. (**b**) The six IAPP segments (highlighted with horizontal bars in **a**) were synthesized and found to form fibrils, as shown in the electron micrographs above (scale bars are 100 nm). Each of the segments also forms microcrystals, as shown in the light micrographs in the center (scale bars are 50 μm). The structures of the six segments were determined, and each revealed a steric zipper. Resolutions and *R* factors are given below; details are described in **Supplementary Methods**. The electron micrographs of segments HSSNNF and NNFGAIL seem to show both microcrystals and fibrils.

DISCUSSION

Peptide polymorphs, prion strains and amyloid polymorphs

Our determination of molecular structures for polymorphic short segments falls far short of revealing the molecular structures for the entire polymorphic fibrils themselves. Solid-state NMR, hydrogen-deuterium exchange, cryo-electron microscopy and other methods[10–12,14,16,18,19,30] have elucidated some fibrous molecular structures, but not yet the atomic structures associated with strains. The highest-resolution view to date of a prion fibril is that of HET-s[31], in which the side chains protruding from pairs of β-strands interdigitate, much like the side chains within steric zippers. That the structures of full proteins in fibrils are more complicated than the structures of short segments is certain: amyloid proteins generally have more than a single segment that forms a steric zipper, and thus protein fibrils may contain more than a single type of β-sheet. In fact, one strain might differ from another in part by the order in which the various steric zippers are nucleated. The variety of steric zippers formed by IAPP (**Fig. 2**) gives a glimpse of the complexity of fibrous states that even a small protein can show. However, even before the complexity of prion strains is fully understood, the models for polymorphism reported here offer one basis for thinking about conformations of prion strains at the molecular level.

A similarity between the polymorphic segment structures reported here, and actual prion strains and amyloid polymorphs of full proteins, is that different conformations arise from different environmental conditions. For example, different strains of Sup35-NM can be produced by incubation at different temperatures[32]. Similarly, distinct polymorphs of Alzheimer's β-amyloid fibrils can be produced by either agitating the dissolved precursor or not agitating[10]. In our case, the polymorphs were produced under different solution conditions. In cells, different environmental conditions might arise from differential hydration, oxidative or xenobiotic stress.

Lastly, the disruptive effect of proline scanning to fibrillation propensity is similar between peptide fibrils and full-length amyloid proteins and prions. When proline residues from the nonfibrillizing mouse IAPP sequence were substituted into these fibrillizing segments from human IAPP, the segments no longer formed fibrils. Three segments with proline replacements were tested: PPTNVG, PPTNVGSNTY and PVLPPT. None of these segments formed fibrils or microcrystals over a period of a year. These observations strengthen the relevance of the short segments whose structures are presented here to the behavior of fibrils of the full protein.

Information transfer in biology

The results presented here suggest that the protein-encoded information transfer associated with prion strains shows similarities to nucleic acid–encoded information transfer in chromosomal inheritance (**Table 3**). The molecular basis for microbial strains is

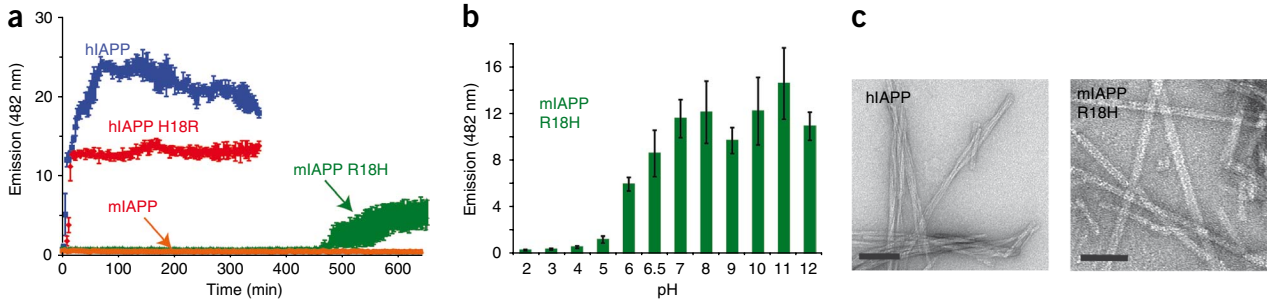

Figure 3 Evidence for at least two steric zipper polymorphs in full-length IAPP. (**a**) Mouse IAPP (mIAPP) does not form fibrils, in contrast to human IAPP (hIAPP), which rapidly forms fibrils. The mutation of Arg18 to histidine in mIAPP permits mIAPP R18H to form fibrils. (**b**) The pH dependence of mIAPP R18H fibrillization supports the involvement of His18. The error bars indicate the s.d. of six replicates. (**c**) hIAPP fibrils are commonly twisted and ~8 nm in width; mIAPP R18H fibrils are uniformly wider (9–10 nm) and untwisted (scale bars are 50 nm), suggesting a different underlying structure.

Table 3 Comparison of molecular mechanisms of inheritance

	Nucleic acid encoded	Protein encoded
Encoding elements	DNA or RNA sequence	Steric zipper structure
Sequence dependent?	Yes	Yes
Recognition method	Base pairing	Amino acid side chain complementarity
Backbone stability	Covalent sugar-phosphate	High-density hydrogen bonding
Information content	Virtually unlimited	Potentially large
Adaptive advantages	High stability and information content	Rapid adaptation to environmental changes

inherent in the central dogma of molecular biology: changes in gene sequence are translated into changes in protein structure, altered catalysis or interactions account for changed phenotypes of the mutant strains, and the phenotypes are heritable because the altered genes are inherited. In contrast, the prion hypothesis[1]—that a protein conformation can define a transmissible or heritable phenotype—was slow to be accepted, because the notion that multiple protein conformations can be heritable or transmissible fell outside common scientific experience. Proteins such as hemoglobin having alternative conformations have long been known. But the energy barriers between the conformations are low, and there was no known way that a conformation could be stabilized during the transmission to progeny cells. To achieve a high energy barrier between conformations, there must be a strong noncovalent force that holds the protein in each distinctive conformation during the process of transmission.

The recognition that prion proteins can enter an amyloid-like, fibrillar state[7,33–35] offers a molecular mechanism for a stabilized, enduring conformation: the fibrillar state is maintained by a high density of hydrogen bonds[36]. More recently, we found that amyloid and prion-derived fibrils have a steric zipper spine that is also maintained by strong van der Waals forces between the sheets[20,21] and strong electrostatic polarization[37]. The strong van der Waals forces bond self-complementary protein sequences, so that the interaction is sequence specific. Prion and amyloid-like fibrils are stable under physiological conditions, so that fibrils can be transmitted to progeny cells. Also, because a protein fibril introduced into a solution of the same protein can seed the dissolved molecules into fibrils, there is an evident molecular mechanism for prion conversion based on fibril properties[38].

Amyloid fibrils have the capacity to carry the information of prion strains because they are polymorphic; the same protein can form a variety of distinct fibril types[8–11,14,16,30]. Yet the molecular mechanism of fibril polymorphism has remained obscure. One proposal, for the specific case of Aβ(1–40) fibrils, is that one polymorph is dimeric and the other trimeric[16]. But because prion strains and fibril morphologies are so varied[6,39], there must be molecular mechanisms that are capable of encoding not just two polymorphs, but many.

The results present here suggest that the molecular basis of fibril polymorphism is based on the large variety of steric-zipper amyloid spines that can form from a single protein. These mechanisms are summarized in **Figure 4**. Considering the possible variety of packing arrangements and segmental and combined structures for steric zippers, it is clear that a substantial variety of prion strains associated with a single protein can be encoded by steric zippers. Although combinatorial polymorphism has not yet been observed on the atomic level, biochemical evidence suggests that it operates in Sup35 fibril polymorphism[14,15,17].

The molecular aspects of the transfer of genetic information by the familiar mechanism of nucleic acid inheritance show similarities to the less familiar protein-based mechanism suggested here for prion strains. In both cases, transfer is by noncovalent bonding. In nucleic acid inheritance, information transfer is achieved by base-pairing, involving complementary hydrogen bonding between bases. In the mechanisms proposed here for prion strains, information transfer is achieved largely by the steric fit (van der Waals bonding) of short, self-complementary amino acid sequences, with hydrogen bonding maintaining the zipper spine. Both mechanisms are sequence specific, based on nucleic acid sequences or self-complementary protein sequences. In the case of prions and amyloid proteins, hydrogen bonds maintain the integrity of the spine, whereas in the case of nucleic acids, covalent bonds maintain the integrity of the backbone. The greater integrity of the covalent backbone of nucleic acids provides a more robust mechanism for ensuring the continuity of life. Although the variation possible in protein-encoded inheritance is small compared to that in genomic DNA, the number of possible steric zippers is enormous. Though less structurally robust and more restricted in information content, protein-based inheritance could allow more rapid responses to environmental changes than do Mendelian mechanisms[40]. In short, the steric zipper presents an alternative model of information transfer

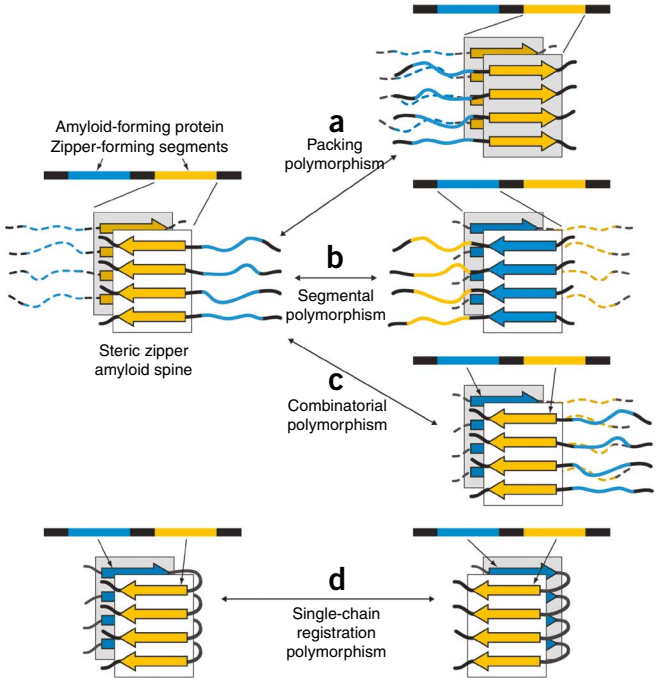

Figure 4 Schematic summary of steric zipper mechanisms for amyloid and prion polymorphism. On the left, an amyloid-forming protein is depicted with two segments (blue and yellow), each capable of forming a self-complementary steric zipper. Below the linear sequence is shown a steric zipper formed by the yellow segment with two β-sheets face to face. (**a**) Packing polymorphism, in which the yellow segment has a sequence capable of forming a second steric zipper with the two β-sheets packing face to back as well as face to face. (**b**) Segmental polymorphism, in which both the yellow and blue segments have sequences capable of forming self-complementary steric zippers. (**c**) Combinatorial polymorphism, in which the blue and yellow segments have sequences capable of engaging in a steric zipper. (**d**) Single-chain registration polymorphism, in which two segments of the same chain form two steric zippers with different registrations of their side chains. Compare this to **Figure 1a,b**, where the registration polymorphs are formed from identical segments of different chains. Neither combinatorial nor single-chain registration polymorphisms have yet been observed at atomic resolution.

that seems to have been adopted by a few microbial and mammalian proteins, and perhaps many others yet to be discovered[41].

METHODS

Methods and any associated references are available in the online version of the paper at http://www.nature.com/nsmb/.

Accession codes. Protein Data Bank: Coordinates and structure factors have been deposited under accession codes 3FVA (NNQNTF), 3FQP (VQIVYK form 2), 3FR1 (NFLVHS), 3FTH (NFLVHSS), 3FPO (HSSNNF), 3FOD (AILSST), 3FTR (SSTNVG form 2), 3FTK (NVGSNTY form 1) and 3FTL (NVGSNTY form 2).

Note: Supplementary information is available on the Nature Structural & Molecular Biology website.

ACKNOWLEDGMENTS

We thank the NE-CAT beamline at the Advanced Photon Source and ID-13 beamline at the European Synchrotron Radiation Facility for beam time and collection assistance, and the National Science Foundation, National Institutes of Health and Howard Hughes Medical Institute for financial support, and P. Chien for discussion.

AUTHOR CONTRIBUTIONS

J.J.W.W., M.L., R.N., M.I.A. and M.R.S. planned, executed and analyzed the research and coauthored the paper; L.G. planned and analyzed the research; A.B.S. executed and analyzed the research; D.C. and K.R. collected the X-ray diffraction data; and D.E. supervised the research and coauthored the paper.

Published online at http://www.nature.com/nsmb/.
Reprints and permissions information is available online at http://npg.nature.com/reprintsandpermissions/.

1. Prusiner, S.B. Prions. *Proc. Natl. Acad. Sci. USA* **95**, 13363–13383 (1998).
2. Chien, P., Weissman, J.S. & DePace, A.H. Emerging principles of conformation-based prion inheritance. *Annu. Rev. Biochem.* **73**, 617–656 (2004).
3. Wickner, R.B., Edskes, H.K., Shewmaker, F. & Nakayashiki, T. Prions of fungi: inherited structures and biological roles. *Nat. Rev. Microbiol.* **5**, 611–618 (2007).
4. Ross, E.D., Minton, A. & Wickner, R.B. Prion domains: sequences, structures and interactions. *Nat. Cell Biol.* **7**, 1039–1044 (2005).
5. Collinge, J., Sidle, K.C., Meads, J., Ironside, J. & Hill, A.F. Molecular analysis of prion strain variation and the aetiology of 'new variant' CJD. *Nature* **383**, 685–690 (1996).
6. Legname, G. *et al.* Continuum of prion protein structures enciphers a multitude of prion isolate-specified phenotypes. *Proc. Natl. Acad. Sci. USA* **103**, 19105–19110 (2006).
7. Caughey, B. & Chesebro, B. Prion protein and the transmissible spongiform encephalopathies. *Trends Cell Biol.* **7**, 56–62 (1997).
8. Tanaka, M., Chien, P., Naber, N., Cooke, R. & Weissman, J.S. Conformational variations in an infectious protein determine prion strain differences. *Nature* **428**, 323–328 (2004).
9. King, C.Y. & Diaz-Avalos, R. Protein-only transmission of three yeast prion strains. *Nature* **428**, 319–323 (2004).
10. Petkova, A.T. *et al.* Self-propagating, molecular-level polymorphism in Alzheimer's β-amyloid fibrils. *Science* **307**, 262–265 (2005).
11. Goldsbury, C.S. *et al.* Polymorphic fibrillar assembly of human amylin. *J. Struct. Biol.* **119**, 17–27 (1997).
12. Jones, E.M. & Surewicz, W.K. Fibril conformation as the basis of species- and strain-dependent seeding specificity of mammalian prion amyloids. *Cell* **121**, 63–72 (2005).
13. Lundmark, K., Westermark, G.T., Olsen, A. & Westermark, P. Protein fibrils in nature can enhance amyloid protein A amyloidosis in mice: Cross-seeding as a disease mechanism. *Proc. Natl. Acad. Sci. USA* **102**, 6098–6102 (2005).
14. Krishnan, R. & Lindquist, S.L. Structural insights into a yeast prion illuminate nucleation and strain diversity. *Nature* **435**, 765–772 (2005).
15. Tessier, P.M. & Lindquist, S. Prion recognition elements govern nucleation, strain specificity and species barriers. *Nature* **447**, 556–561 (2007).
16. Paravastu, A.K., Leapman, R.D., Yau, W.M. & Tycko, R. Molecular structural basis for polymorphism in Alzheimer's β-amyloid fibrils. *Proc. Natl. Acad. Sci. USA* **105**, 18349–18354 (2008).
17. Chang, H.Y., Lin, J.Y., Lee, H.C., Wang, H.L. & King, C.Y. Strain-specific sequences required for yeast [PSI+] prion propagation. *Proc. Natl. Acad. Sci. USA* **105**, 13345–13350 (2008).
18. Madine, J. *et al.* Structural insights into the polymorphism of amyloid-like fibrils formed by region 20–29 of amylin revealed by solid-state NMR and X-ray fiber diffraction. *J. Am. Chem. Soc.* **130**, 14990–15001 (2008).
19. Sachse, C., Fandrich, M. & Grigorieff, N. Paired beta-sheet structure of an Abeta (1–40) amyloid fibril revealed by electron microscopy. *Proc. Natl. Acad. Sci. USA* **105**, 7462–7466 (2008).
20. Nelson, R. *et al.* Structure of the cross-β spine of amyloid-like fibrils. *Nature* **435**, 773–778 (2005).
21. Sawaya, M.R. *et al.* Atomic structures of amyloid cross-beta spines reveal varied steric zippers. *Nature* **447**, 453–457 (2007).
22. Wiltzius, J.J. *et al.* Atomic structure of the cross-β spine of islet amyloid polypeptide (amylin). *Protein Sci.* **17**, 1467–1474 (2008).
23. Höppener, J.W., Ahren, B. & Lips, C.J. Islet amyloid and type 2 diabetes mellitus. *N. Engl. J. Med.* **343**, 411–419 (2000).
24. von Bergen, M. *et al.* Assembly of tau protein into Alzheimer paired helical filaments depends on a local sequence motif ((306)VQIVYK(311)) forming beta structure. *Proc. Natl. Acad. Sci. USA* **97**, 5129–5134 (2000).
25. Sigurdson, C.J. *et al.* De novo generation of a transmissible spongiform encephalopathy by mouse transgenesis. *Proc. Natl. Acad. Sci. USA* **106**, 304–309 (2009).
26. Sunde, M. *et al.* Common core structure of amyloid fibrils by synchrotron X-ray diffraction. *J. Mol. Biol.* **273**, 729–739 (1997).
27. Nishi, M., Chan, S.J., Nagamatsu, S., Bell, G.I. & Steiner, D.F. Conservation of the sequence of islet amyloid polypeptide in five mammals is consistent with its putative role as an islet hormone. *Proc. Natl. Acad. Sci. USA* **86**, 5738–5742 (1989).
28. Betsholtz, C. *et al.* Sequence divergence in a specific region of islet amyloid polypeptide (IAPP) explains differences in islet amyloid formation between species. *FEBS Lett.* **251**, 261–264 (1989).
29. Green, J. *et al.* Full-length rat amylin forms fibrils following substitution of single residues from human amylin. *J. Mol. Biol.* **326**, 1147–1156 (2003).
30. Tanaka, M., Collins, S.R., Toyama, B.H. & Weissman, J.S. The physical basis of how prion conformations determine strain phenotypes. *Nature* **442**, 585–589 (2006).
31. Wasmer, C. *et al.* Amyloid fibrils of the HET-s(218–289) prion form a beta solenoid with a triangular hydrophobic core. *Science* **319**, 1523–1526 (2008).
32. Tanaka, M., Chien, P., Yonekura, K. & Weissman, J.S. Mechanism of cross-species prion transmission: an infectious conformation compatible with two highly divergent yeast prion proteins. *Cell* **121**, 49–62 (2005).
33. Prusiner, S.B. *et al.* Scrapie prions aggregate to form amyloid-like birefringent rods. *Cell* **35**, 349–358 (1983).
34. Come, J.H., Fraser, P.E. & Lansbury, P.T. Jr. A kinetic model for amyloid formation in the prion diseases: importance of seeding. *Proc. Natl. Acad. Sci. USA* **90**, 5959–5963 (1993).
35. Glover, J.R. *et al.* Self-seeded fibers formed by Sup35, the protein determinant of [PSI+], a heritable prion-like factor of *S. cerevisiae*. *Cell* **89**, 811–819 (1997).
36. Pauling, L. & Corey, R.B. The pleated sheet, a new layer configuration of polypeptide chains. *Proc. Natl. Acad. Sci. USA* **37**, 251–256 (1951).
37. Tsemekhman, K., Goldschmidt, L., Eisenberg, D. & Baker, D. Cooperative hydrogen bonding in amyloid formation. *Protein Sci.***16**, 761–764 (2007).
38. Jarrett, J.T. & Lansbury, P.T. Jr. Seeding "one-dimensional crystallization" of amyloid: a pathogenic mechanism in Alzheimer's disease and scrapie? *Cell* **73**, 1055–1058 (1993).
39. Meinhardt, J., Sachse, C., Hortschansky, P., Grigorieff, N. & Fandrich, M. Abeta (1–40) fibril polymorphism implies diverse interaction patterns in amyloid fibrils. *J. Mol. Biol.* **386**, 869–877 (2009).
40. Shorter, J. & Lindquist, S. Prions as adaptive conduits of memory and inheritance. *Nat. Rev. Genet.* **6**, 435–450 (2005).
41. Alberti, S., Halfmann, R., King, O., Kapila, A. & Lindquist, S. A systematic survey identifies prions and illuminates sequence features of prionogenic proteins. *Cell* **137**, 146–158 (2009).
42. Thompson, M.J. *et al.* The 3D profile method for identifying fibril-forming segments of proteins. *Proc. Natl. Acad. Sci. USA* **103**, 4074–4078 (2006).

ONLINE METHODS

Amyloid propensity prediction. We predicted fibril formation propensities for human and mouse IAPP sequences using the 3D Profile method[42]. This algorithm uses the amyloid-like crystal structure of the NNQQNY segment[20] as a structural template. Each six-residue, proline-free segment sequence is threaded onto the NNQQNY backbone structure, and the energetic fit is evaluated using the RosettaDesign program[43]. Given the energies of experimentally determined amyloid-like segments, we chose an energy threshold for fibril formation propensity of –23 kcal mol^{-1}. That is, segments with computed energies equal to or below this threshold were deemed to have high propensity to form fibrils. The energies of all hexameric segments in IAPP were plotted, assigning the computed energy to the first residue of the hexameric segment (**Fig. 2a**).

Crystallization and structure determination. All peptide segments (custom synthesis, CS Bio) were crystallized using the hanging drop–vapor diffusion method. Details of crystallization, structure determination and refinement for each of the novel structures are provided in **Supplementary Methods**.

Fibril formation. Lyophilized segments were dissolved to 1 mM in 100% hexafluoroisopropanol and then diluted to 10 μM in 20 μM sodium acetate at pH 6.5 (final, 1% (v/v) hexafluoroisopropanol). Fibril formation was monitored by thioflavin T fluorescence at 450 nm excitation and 482 nm emission wavelengths. Data were collected in triplicate; error bars show the s.d. between samples. For the experiments conducted as a function of pH, samples were allowed to incubate at least 1 d; the final thioflavin T fluorescence signal averaged for at least three samples is shown for comparison. The quiescent samples were incubated with 10 μM thioflavin T at 37 °C in various buffer conditions for appropriate pH. The measured presence or absence of fibrils was confirmed by negative-stain electron microscopy (data not shown).

43. Liu, Y. & Kuhlman, B. RosettaDesign server for protein design. *Nucleic Acids Res.* **34**, W235–W238 (2006).